THE JOURNAL OF BIOLOGICAL CHEMISTRY VOL. 284, NO. 30, pp. 19927–19936, July 24, 2009

S156C Mutation in Tissue Inhibitor of Metalloproteinases-3 Induces Increased Angiogenesis*

Received for publication, April 27, 2009 Published, JBC Papers in Press, May 28, 2009, DOI 10.1074/jbc.M109.013763

Jian Hua Qi[‡], Ganying Dai[‡], Philip Luthert[§], Shyam Chaurasia[‡], Joe Hollyfield[‡], Bernhard H. F. Weber[¶], Heidi Stöhr[¶], and Bela Anand-Apte[‡‖1]

From the [‡]Department of Opthalmology, Cole Eye Institute and the [‖]Department of Molecular Medicine, Cell Biology, Cleveland Clinic Lerner College of Medicine at Case Western Reserve University, Cleveland, Ohio 44195, the [§]Department of Pathology, Institute of Ophthalmology, London, England, and the [¶]Institute of Human Genetics, University of Regensburg, 93053 Regensburg, Germany

Tissue Inhibitor of metalloproteinases-3 (TIMP-3) is a potent matrix-bound angiogenesis inhibitor. Mutations in TIMP-3 cause Sorsby Fundus Dystrophy, a dominant inherited, early onset macular degenerative disease, with choroidal neovascularization causing a loss of vision in the majority of patients. Here we report that expression of S156C TIMP-3 mutation in endothelial cells results in an abnormal localization of the protein, increased glycosylation, decreased matrix metalloproteinase inhibitory activity, and increased vascular endothelial growth factor (VEGF) binding with a consequent increase in VEGF-dependent migration and tube formation. These enhanced signaling events appear to be mediated as a consequence of a post-transcriptionally regulated increase in the expression of membrane-associated VEGFR-2 in endothelial cells of *Timp-3*$^{156/156}$ mutant mice as well as in human Sorsby fundus dystrophy eyes. Understanding the mechanism(s) by which mutant TIMP-3 can induce abnormal neovascularization provides important insight into the pathophysiology of a number of diseases with increased angiogenesis.

Tissue inhibitor of metalloproteinases-3 (TIMP-3)[2] is a member of the TIMP family of proteins and is an endogenous inhibitor of matrix metalloproteinases (MMPs), a disintegrin and metalloproteinase (ADAM), and ADAM with thrombospondin domains (ADAMTS) family of enzymes. TIMP-3 is unique among other members of the TIMP family in that it is tightly bound to the extracellular matrix (ECM). In addition, TIMP-3 is the only TIMP that can inhibit tumor necrosis factor α-converting enzyme (TACE/ADAM17) and aggrecanase 1 and 2 (ADAMTS4 and ADAMTS5). Functionally, apart from being a key inhibitor of MMPs (1, 2) and regulating apoptosis in some cells *in vitro* and *in vivo* (3–7), TIMP-3 has been demonstrated to be a potent inhibitor of angiogenesis through its ability to block the binding of VEGF to its receptor VEGFR-2 (also known as KDR and FLK-1), affecting subsequent receptor downstream signaling (8). TIMP-3 protein is produced constitutively by the retina pigment epithelium (RPE) and choroidal endothelial cells (9, 10) in the eye and is a component of the normal Bruch membrane (11). Sorsby fundus dystrophy (SFD) (12), a dominantly inherited, degenerative disease of the macula, is caused by specific mutations in the *TIMP-3* gene (13–20), most of which introduce an unpaired cysteine at the C terminus of the protein. SFD is of considerable interest as it is the only genetic disorder in which choroidal neovascularization occurs in the majority of affected patients (21–23). SFD-TIMP-3 protein accumulates in deposits in Bruch membrane (24) and shows pro-apoptotic activity (25) and reduced MMP inhibitory activity (10). Whether SFD-TIMP-3 affects VEGFR-2-mediated VEGF signaling specific to angiogenesis is unknown. In this study we have generated endothelial cells (ECs) expressing SFD-related S156C TIMP-3 mutation as a platform and determined how mutant TIMP-3 regulates VEGF signaling via VEGFR-2 during SFD-related angiogenesis. In addition, we have analyzed retinas from mice carrying the related S156C mutation and a postmortem human eye with SFD to confirm our experimental results.

EXPERIMENTAL PROCEDURES

Materials—Porcine aortic endothelial (PAE and PAE$_{KDR}$) cells were cultured in Ham's F-12/Dulbecco's modified Eagle's medium supplemented with 10% fetal bovine serum (Hyclone, Logan, UT), 50 unit/ml penicillin, and 50 μg/ml streptomycin as described previously (10). Recombinant human VEGF was a kind gift from Genentech. Antibodies were monoclonal anti-TIMP-3 antibody (Chemicon International, Inc., Temecula, CA), monoclonal anti-Flk-1 (A-3), goat polyclonal anti-actin (C-11), and bovine anti-goat lgG-horseradish peroxidase (Santa Cruz Biotechnology, Santa Cruz, CA)), polyclonal phospho-VEGF receptor-2/3 (Ab-1) antibody (Oncogene™ Research Products, Cambridge, MA), monoclonal anti-VEGF receptor-2 (KDR), clone KDR-2, (Sigma), mitogen-activated protein kinase (MAPK), and phospho-specific MAPK antibodies (Calbiochem-Novabiochem), and horseradish peroxidase-conju-

* This work was supported, in whole or in part, by National Institutes of Health Grants EY016490, CA106415, and EY015638. This work was also supported by a Foundation Fighting Blindness Center grant, a Research to Prevent Blindness (RPB) Challenge grant, an Ohio Biomedical Research and Technology Transfer Partnership Program 05-29 and RPB Lew Wasserman award (to B. A.-A.), and Grant STO 366/3-1 from the Deutsche Forschungsgemeinschaft (to H. S.).

[1] To whom correspondence should be addressed: Dept. of Ophthalmology, Cole Eye Institute i3-161, Cleveland Clinic, 9500 Euclid Ave., Cleveland, OH 44195. Tel.: 216-445-9739; Fax: 216-445-3670; E-mail: anandab@ccf.org.

[2] The abbreviations used are: TIMP-3, tissue inhibitor of metalloproteinases-3; SFD, Sorsby fundus dystrophy; ADAM, a disintegrin and metalloproteinase; ECM, extracellular matrix; RPE, retina pigment epithelium; EC, endothelial cell; CM, conditioned medium; MMP, matrix metalloproteinase; VEGFR, vascular endothelial growth factor (VEGF) receptor; PAE, porcine aortic endothelial; RT, reverse transcription; PBS, phosphate-buffered saline; WT, wild type; ERK, extracellular signal-regulated kinase.

gated anti-rabbit and anti-mouse IgG antibodies (GE Healthcare). Post-mortem control non-diseased age-matched eyes were obtained from National Disease Research Interchange, National Resource Center, Philadelphia.

Generation of EC Cell Lines Expressing Wild-type or S156C Mutant TIMP-3—A 550-bp Timp-3 or S156C Timp-3 insert from a human cDNA clone was cloned into expression vector pCEP4 (Invitrogen). PAE_{KDR} cells were transfected with Timp-3 cDNA (WT or mutant) or empty vector using Lipofectamine reagent (Invitrogen). Stable clones were isolated using hygromycin selection. RT-PCR, Western blot, and reverse zymography were used to identify and analyze the expression of TIMP-3 or mutant TIMP-3, respectively.

RT-PCR—Total RNA was extracted from the cells by using Totally RNA™ kit (Ambion Inc., Austin, Texas). RT-PCR was performed using a RETROscript™ First Strand Synthesis kit (Ambion). 10 ng of total RNA was used for RT and amplification. The sequences of the PCR primer pairs for human VEGFR-2 and TIMP-3 gene were 5′-CTT CGA AGC ATC AGC ATA AGA AAC T-3′ (forward) and 5′-TGG TCA TCA GCC CAC TGG AT-3′ (reverse) and 5′-CTC TGC AAC TCC GAC ATC GTG AT-3′ (forward) and 5′-CAG CAG GTA CTG GTA CTT GTT GAC-3′ (reverse), respectively. 28 S primers (forward, 5′-GTT CAC CCA CTA ATA GGG AAC GTG A-3′, and reverse, 5′-GAT TCT GAC TTA GAG GCG TTC AGT-3′) were used as a control for RNA expression. PCR conditions were 94 °C for 3 min followed by 30 cycles (94 °C, 30 s; 55 °C, 30 s; 72 °C, 1 min) and a final extension step of 72 °C for 5. Real-time PCR was performed to compare the levels of VEGFR-2 in endothelial cells expressing WT or mutant TIMP-3. Complementary DNA was synthesized by reverse transcription of total RNA (1 μg) using the iScript cDNA synthesis kit (Bio-Rad). Real time PCR was performed on a DNA Engine Opticon™ system (MJ Research/GMI, Ramsey, MN) using brilliant SYBR green kit with a thermal profile of 94 °C for 2 min followed by 40 cycles of 94 °C for 30 s, 55 °C for 30 s, and 72 °C for 1 min. Results are expressed as C_T values, where C_T is defined as the cycle number at which an increase above background fluorescence could be reliably detected, and ΔC_T is the difference between the C_T values of KDR and 28 S. Vector PAE/KDR cDNA was used as calibrator to generate a $\Delta\Delta C_T$ value (ΔC_T WT or mutant PAE/KDR sample-ΔC_T vector sample). The -fold differential expression in KDR compared with calibrator was expressed as $2^{-\Delta\Delta CT}$.

Preparation of Cellular Fractions—2-Day serum-free-conditioned medium (CM) was collected from subconfluent cells cultured on six-well plates. In some cases the CM was further concentrated with heparin-agarose gels (Bio-Rad). The cell monolayer was dislodged from the culture plates after a 10-min incubation in Ca^{2+}-, Mg^{2+}-free phosphate-buffered saline (PBS) containing 2.5 mM EDTA. After several rinses in PBS and water, the ECM was scraped in a small volume of electrophoresis sample buffer without reducing agent for analyses.

Ligand Binding Assay—1×10^6 cells/well in 12-well plates were incubated with the indicated concentrations of ^{125}I-$VEGF_{165}$ (specific activity, 1805 Ci/mmol, GE Healthcare) in the presence or absence of a 50-fold excess of unlabeled VEGF for 2 h on ice. After washing, the cell monolayers were solubilized with lysis buffer (20 mM Tris HCl, pH 7.5, 1% Triton X-100, and 10% glycerol), and the radioactivity was measured in a gamma counter.

Immunoprecipitation and Immunoblotting—Cell fractions or immunoprecipitates of the lysates with the indicated antibodies were subjected to SDS-PAGE. Proteins were probed with antibody and detected with either a horseradish peroxidase-conjugated anti-rabbit or anti-mouse IgG antibody (Amersham) followed by ECL. The blots were re-stripped with Western ReProbe™ solution (GBiosciences, Maryland Heights, MO) for 30 min and reprobed as indicated.

Reverse Zymography—Conditioned medium, cell lysates, and ECM fractions from transfected cells were prepared as described previously (10). Equal amounts of protein were loaded onto a 12% gel with 1 mg/ml gelatin plus RPE cell-conditioned media, as a source of MMPs, for reverse zymography and processed as described previously (2).

Immunofluorescence Staining—For immunostaining, subconfluent cells cultured on Falcon culture slides (BD, Biosciences) were used. For actin reorganization, cells were stimulated for 15 min at 37 °C with 50 ng/ml VEGF or control buffer. The cells were fixed with 3.7% paraformaldehyde in PBS for 30 min at 4 °C and permeabilized with 0.2 Triton X-100 for 20 min at room temperature. After rinsing with PBS the cells were incubated with fluorescein isothiocyanate-labeled phalloidin in PBS (0.66 μg/ml, Sigma) for 20 min at room temperature, washed with PBS, and analyzed by fluorescence microscopy.

Proliferation Assay—Cells were seeded at a density of 5000 cells/well in 24-well culture plates and cultured for 24 h in growth medium. After synchronization overnight in serum-free medium supplemented with 0.1% BSA (Sigma), cells were stimulated with or without VEGF for 36 h followed by the addition of 0.4 μCi/ml [^{3}H]thymidine for 4 h. High molecular weight DNA was precipitated using 5% trichloroacetic acid at 4 °C for 30 min. After two washes with ice-cold H_20, ^{3}H radioactivity was solubilized in 1 N NaOH for 20 min at room temperature, acidified by the addition of 2 N HCl, and measured using a liquid scintillation counter. Each sample was assayed in triplicate, and the assays were repeated at least twice.

Migration Assay—A modified Boyden chamber assay was carried out as described previously (8). Briefly, 8.0-μm pore polyvinylpyrrolidone free polycarbonate membranes were precoated with 100 μg/ml collagen type I in 0.2 N acetic acid (Cohesion Technologies, Palo Alto, CA). VEGF at the indicated concentrations was placed in the lower chamber, and cells (2×10^6) in serum-free medium were placed in the upper chambers. The chamber was then incubated for 4 h at 37 °C in a 5% CO_2-humidified incubator. Cells remaining on the top of the filter were removed. Cells on the bottom surface of the filter were fixed, stained, and mounted. The number of migrating cells per well was counted microscopically.

Tube Formation Assay—Type 1 collagen was mixed with 10× Dulbecco's modified Eagle's medium and 0.1 M NaOH (8:1:1), adjusted to a solution containing 10 μg/ml growth factor-reduced Matrigel matrix (BD Biosciences), and then distributed in 48-well dishes. After gelling, serum-starved cells were seeded on the collagen gels at 1.5×10^4 cells/well and maintained in

serum-free medium in the presence or absence of 50 ng/ml VEGF. After 4 h of incubation at 37 °C, a second layer of collagen was added, and cultures were kept under the same conditions as described above. Tube formation was examined using a phase-contrast microscopy at the indicated time points.

Immunohistochemistry—For staining frozen sections, slides were fixed in cold acetone for 10 min and blocked with 10% goat serum in PBS containing 0.2% Triton X-100 for 1 h. Anti-VEGFR-2 (1: 200) was then applied. After an overnight incubation at 4 °C, the antibody binding was resolved with Alexa Fluor 488-conjugated goat anti-mouse lgG (Invitrogen Molecular Probes) or Texas Red-conjugated AffiniPure goat anti-mouse lgG (Jackson ImmunoResearch Laboratories). Specificity of the immunostaining was verified by substituting the primary antibody with an equivalent dilution of a nonspecific control mouse lgG. Slides were mounted in antifade medium containing 4′,6-diamidino-2-phenylindole for labeling nuclei (Vectashield; Vector Laboratories, Inc., Burlingame, CA). Images were taken with a confocal laser-scanning microscope or a fluorescence microscope. For staining of paraffin sections, slides were deparaffinized in xylene and rehydrated through an alcohol series. Endogenous peroxidase was blocked by immersion in 0.3% hydrogen peroxidase for 30 min. No antigen retrieval was required except for factor VIII staining. Antibodies against TIMP-3, VEGFR-2, and factor VIII (dilution 1: 200) were applied overnight at 4 °C. The sections were processed further using a Vectastain ABC kit and VectorR VIP substrate kit for peroxidase (Vector Laboratories). Control sections were processed in the same way with negative control rabbit and mouse lgG.

Statistical Analysis—The *p* values were calculated from Student's *t* test or analysis of variance using comparisons with control samples tested at the same time.

RESULTS

S156C TIMP-3 Is Abnormally Distributed in Endothelial Cells—Stable endothelial cell lines (PAE_{KDR}) expressing wild-type (WT) or S156C mutant *TIMP-3* cDNA or vector alone were generated. Two independent clones expressing similar levels of mRNA (identified by RT-PCR) encoding WT (W1, W4) or mutant TIMP-3 (M7, M10) were identified (Fig. 1*A*). Western blot analysis using monoclonal antibodies against TIMP-3 determined that in endothelial cells WT TIMP-3 was predominantly localized in the ECM in a 23-kDa form (Fig. 1*B*, *upper panel*) with a very small fraction secreted into the CM (Fig. 1*B*, *lower panel*), confirming previous reports that TIMP-3 is an ECM-bound protein in endothelial cells (8). On the other hand, mutant Ser-156 TIMP 3 was detected predominantly in the CM as a 28-kDa protein (Fig. 1*B*), suggesting a possible reduced ECM binding property for the mutant protein. To determine whether the higher molecular weight form of mutant TIMP-3 was a result of glycosylation, samples were treated with peptide *N*-glycosidase F (an amidase that removes *N*-linked glycoproteins) before analyses. This treatment resulted in a conversion of the 28-kDa form to the 23-kDa form (Fig. 1*C*), which suggests that the 28-kDa protein is a glycosylated variant of mutant TIMP-3. The spatial expression of mutant TIMP-3 and its molecular mass species in endothelial

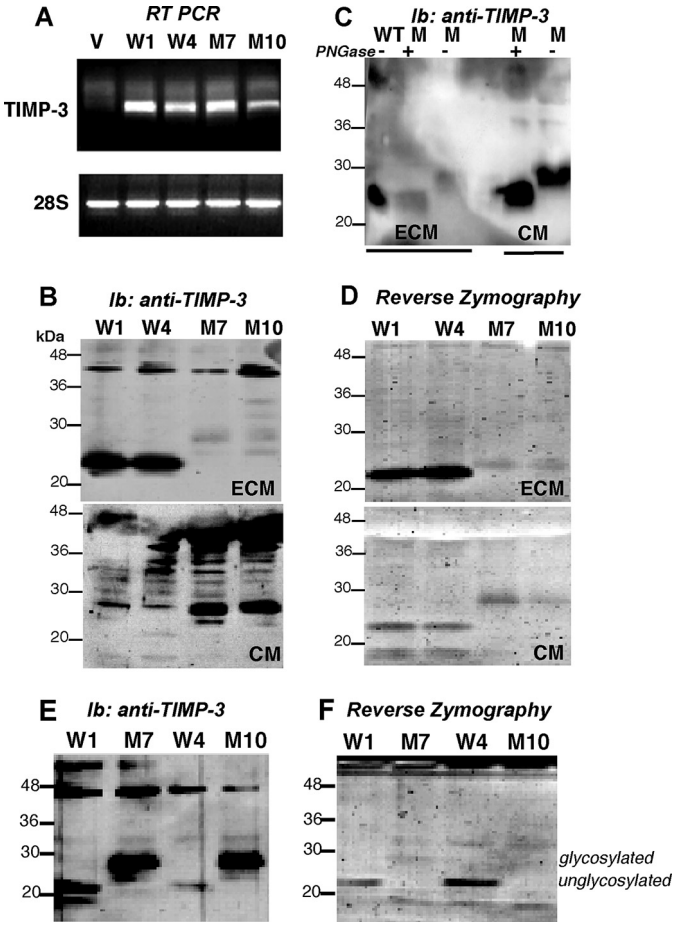

FIGURE 1. **Abnormal localization of S156C TIMP-3 in endothelial cells.** Analysis of WT TIMP-3 (*W1* and *W4*), S156C TIMP-3 (*M7* and *M10*) and control vector-transfected (*V*) PAE_{KDR} cells. *A*, total RNA extracts were analyzed for TIMP-3 and 28S mRNAs by RT-PCR. *B*, the expression levels and cellular localization of WT and S156C TIMP-3 proteins in the ECM and CM were determined by immunoblotting (*Ib*) with anti-TIMP-3 monoclonal antibodies. *C*, the ECM and CM prepared from mutant cells were treated with peptide *N*-glycosidase F (*PGNase*), and deglycosylation was analyzed by immunoblotting with anti-TIMP-3 monoclonal antibody. WT TIMP-3 in the ECM was used as a positive control for the unglycosylated form. *D*, TIMP (MMP inhibitory) activity in the ECM (*upper panel*) and CM (*lower panel*) was analyzed by reverse zymography. *E*, heparin-agarose-conditioned medium from WT and mutant cells was analyzed for TIMP-3 by immunoblotting with TIMP-3 monoclonal antibody. *F*, heparin-agarose-conditioned medium from WT and mutant cells was analyzed for TIMP-3 activity by reverse zymography.

cells are distinct from those observed in RPE cells (10, 26), where the mutant protein is expressed in the ECM like its wild-type counterpart. The reason for this discrepancy is likely because of unique distributions and expressions in different cell types. The MMP inhibitory activity of WT and mutant TIMP-3 was further analyzed by reverse zymography. ECM and CM of PAE_{KDR} cells expressing WT TIMP-3 (W1, W4) showed a marked MMP inhibitory species with an approximate molecular mass of 23 kDa corresponding to the protein visualized on Western blot (Fig. 1*D*). However, the cells expressing mutant TIMP-3 (M7, M10) exhibited minimal MMP inhibitory activity in CM or ECM samples (Fig. 1*D*), similar to our previous observations in RPE cells (10). A similar result was obtained by Western blot analyses (Fig. 1*E*) and reverse zymography (Fig. 1*F*) of heparin-agarose-concentrated CM. These results indicate that mutant Ser-156-TIMP-3 exhibits characteristics of an abnor-

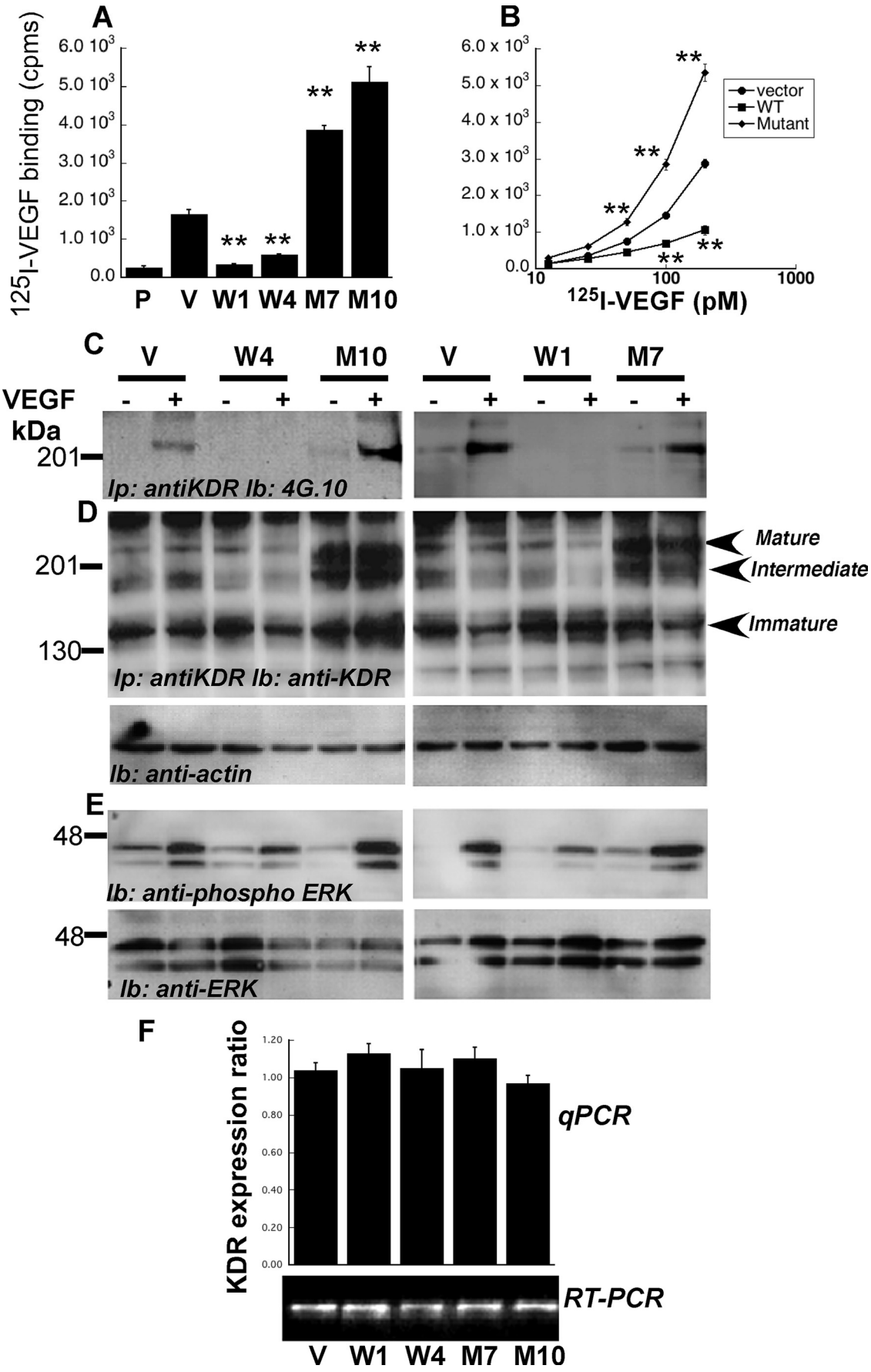

mal protein, including reduced binding to the ECM of endothelial cells in addition to a reduction in MMP inhibitory activity.

S156C TIMP-3 Expression in ECs Increases VEGF Binding to VEGFR-2—To determine whether expression of mutant TIMP-3 regulates the interaction of VEGF with VEGFR-2, we examined VEGF binding in parental PAE and the transfected PAE_{KDR} cell lines using a ^{125}I-VEGF binding assay. Mock cells (Fig. 2, *V*, PAE_{KDR} cells transfected with empty vector) but not parental PAE (*P*, ECs not expressing KDR) cells showed a specific concentration-dependent ^{125}I-VEGF binding (data not shown). As we have shown previously, WT TIMP-3 expression dramatically inhibited the binding of ^{125}I-VEGF to VEGFR-2, with a downward shift of the concentration binding curve (Fig. 2, *A* and *B*). Surprisingly, the expression of mutant TIMP-3 resulted in a 2–3-fold increase in ^{125}I-VEGF binding with an upward shift in the concentration binding curve (Fig. 2, *A* and *B*).

S156C TIMP-3 Expression in ECs Accentuates VEGFR-2 Signaling via Elevated Receptor Levels—Because mutant cells showed an increased VEGF binding to VEGFR-2, we tested whether these cells had elevated levels of functional VEGFR-2 on their surface. Co-immunoprecipitation of VEGFR-2 followed by Western blot analysis using an anti-phosphotyrosine antibody demonstrated that VEGF stimulated the tyrosine phosphorylation of a 210-kDa VEGFR-2 protein in cell lysates prepared from both control transfected cells (*V*) and mutant cells (*M*) (Fig. 2*C*). In contrast, as reported previously, no receptor autophosphorylation was seen in WT TIMP-3 cells (Fig. 2*C*). Immunoprecipitation and Western blot analysis of cell lysates with antibody directed against the C terminus of VEGFR-2 in mock-transfected cells (*V*) showed a mature form of VEGFR-2 corresponding to a molecular size of 210-kDa that phosphorylated in response to VEGF. In addition, two other receptor forms (a 200-kDa intermediate form and smaller fragment (immature form) at ~160 kDa) were also observed that were not phosphorylated (Fig. 2*D*), consistent with previous reports (27). There was a marked increase in intensity of the mature form and intermediate form of the receptor in mutant cells compared with WT TIMP-3 and control cells (Fig. 2*D*). Activation of mitogen-activated protein kinase is a known VEGFR-2 downstream signaling event. We measured the phosphorylation of two mitogen-activated protein kinases, ERK1 (p44) and ERK2 (p42), by Western blot analysis of cell lysates in WT and mutant endothelial cells. VEGF stimulated the phosphorylation of ERK1/2 in mock cells (*V*) and mutant cells (*M*) but not in WT TIMP-3 cells (Fig. 2*E*, *upper panel*), whereas the expression of WT and mutant TIMP-3 had no impact on total ERK1/2 levels (Fig. 2*E*, *lower panel*). These results determine that elevated VEGFR-2 in mutant cells is associated with enhanced activation of ERK1/2 when compared with cells expressing WT TIMP-3. RT-PCR (Fig. 2*F*, *lower panel*) and quantitative PCR analyses (Fig. 2*F*, *upper panel*) determined that mutant TIMP-3 does not up-regulate VEGFR-2/KDR gene expression in endothelial cells. Overall, these data indicate that mutant TIMP-3 potentiates VEGF-stimulated tyrosine phosphorylation of VEGFR-2 via elevated receptor levels on the cell surface.

S156C TIMP-3 Enhances VEGF-stimulated Migration and Actin Reorganization but Not Proliferation—To investigate whether elevated VEGFR-2 signaling in cells expressing mutant TIMP-3 could be translated into enhanced biological responses, we examined VEGF-stimulated proliferation and migration, two critical steps in the angiogenic process, in the transfected PAE_{KDR} cell lines. Quiescent endothelial cells were stimulated with VEGF and evaluated by incorporation of [^{3}H]thymidine. As shown in Fig. 3*A*, *left panel*, VEGF stimulated the proliferation of mock-transfected cells in a concentration-dependent fashion with a maximum activity at 15 ng/ml. Mutant cells exhibited similar mitogenic responses to VEGF, whereas WT TIMP-3 cells showed a dramatic attenuation in the VEGF response (Fig. 3*A*, *right panel*), indicating that cells expressing mutant TIMP-3 is an inefficient inhibitor of VEGF-stimulated EC proliferation.

A mini-Boyden chamber assay was used to examine VEGF-stimulated cell migration. VEGF stimulated a concentration-dependent migratory response in mock cells with a maximum effect at 50 ng/ml (Fig. 3*B*, *left panel*). WT TIMP-3 expression, but not mutant TIMP-3m dramatically reduced basal and VEGF-stimulated migration. Mutant TIMP-3-expressing cells had an accentuated migratory response toward VEGF (Fig. 3*B*, *right panel*). EC migration involves reorganization of the actin cytoskeleton with the formation of membrane edge ruffles that have previously been shown to be an integral part of cellular motility. We analyzed VEGF-stimulated formation of membrane ruffles in the PAE_{KDR} cell lines. Treatment of quiescent cells with VEGF for 15 min resulted in the formation of membrane ruffles in a small percentage of mock-transfected cells (*V*) (Fig. 3*C*), whereas a majority of mutant cells showed more striking edge ruffles (Fig. 3*C*). In contrast, WT TIMP-3 cells (Fig. 3*C*) did not form membrane ruffles in response to VEGF. These data provide convincing evidence that mutant TIMP-3 is an inefficient inhibitor and likely an enhancer of VEGF-induced EC responses.

S156C TIMP-3 Increases Differentiation but Not Survival during VEGF-dependent Tube Formation—An *in vitro* angiogenesis assay using a type 1 collagen substrate was employed to study whether mutant TIMP-3 affected VEGF-stimulated tube formation, which recapitulates the later stages of angiogenesis.

FIGURE 2. **Endothelial cells expressing S156C TIMP-3 have increased levels of VEGFR-2 with increased binding of VEGF.** PAE_{KDR} cells expressing WT (*W*) or S156C TIMP-3 (*M*) or vector alone (*V*) were incubated with or without VEGF and analyzed for VEGF binding. *A*, ^{125}I-$VEGF_{165}$ binding is expressed as cpm/well. *B*, concentration-dependent ^{125}I-$VEGF_{165}$ binding in PAE_{KDR} cells. All results are the mean ± S.D. of a typical experiment. At least three independent experiments gave comparable results. **, $p < 0.01$ *versus* corresponding vector controls. *C*, $VEGF_{165}$-mediated phosphorylation of VEGFR-2 in PAE_{KDR} cells expressing WT (*W*) or S156C TIMP-3 (*M*) or vector alone (*V*). Lysates from cells stimulated or not with 50 ng/ml VEGF for 10 min were separated by SDS-PAGF (10%) and analyzed by immunoprecipitation (*Ip*) with an anti-KDR antibody followed by immunoblotting with an anti-phosphotyrosine antibody, 4G.10. *D*, KDR protein was analyzed by immunoprecipitation and immunoblotting (*Ib*) of cell lysates using anti-KDR antibody (*upper panel*). Immunoblotting of cell lysates with anti-actin antibody (*lower panel*) is shown. *E*, phosphorylation of ERK1 and ERK2 in response to VEGF was detected by immunoblotting with phosphospecific ERK antibodies (*top panel*). Total protein levels of ERK were determined by immunoblotting with anti ERK1/2 antibodies (*bottom panels*). *F*, quantitative (*q*) PCR and RT-PCR for KDR were performed on control vector transfected, WT, and S156C mutant TIMP-3-expressing cells.

In this assay cells were grown in three-dimensional collagen gels in the presence or absence of VEGF for up to 8 days in culture. After 24 h, VEGF stimulated the differentiation of mock cells to form tube-like structures that survived over the 8 days of culture (Fig. 3*D*). In contrast, the ability of WT TIMP-3 cells to form tube-like structures was severely compromised (Fig. 3*D*). However, mutant cells treated with VEGF organized rapidly, forming extensive tubular networks, but by day 5 the tubular structures started to regress and collapse. Both WT TIMP-3 and mutant cells exhibited morphologic features characteristic of cell death relative to mock cells under basal conditions (Fig. 3*D*). These data suggest that mutant TIMP-3 might potentiate RPE-driven angiogenesis by increasing VEGF signaling via elevated VEGFR-2.

Decreased MMP Inhibitory Activity and Increased VEGFR-2 Levels in Timp-3$^{S156C/S156C}$ Mice—Spleen and posterior pole eye tissue from homozygous mice carrying the SFD-associated S156C mutation (28) were analyzed for MMP inhibitory activity and gelatinase activity by reverse zymography and zymography, respectively. Spleen tissue from *Timp-3$^{S156C/S156C}$* mutant mice showed a complete absence of TIMP-3 activity in both 24- and 28-kDa (glycosylated) forms (Fig. 4*a*, *upper panel*) with a corresponding increase in MMP-9 activity (Fig. 4*b*, *upper panel*). Interestingly the TIMP-3 activity in the retinae of *Timp-3$^{S156C/S156C}$* mutant mice was markedly decreased (Fig. 4*a*, *lower panel*), however, with no corresponding increase in MMP-9 (Fig. 5*b*, *lower panel*). It does appear that the remnant 28-kDa MMP inhibitory species seen in the eyes of the mutant mice could likely be other TIMPs (either 28-kDa TIMP-1 or 29-kDa TIMP-4) based on similar bands observed in the retinae of Timp-3 null mice (data not shown). These TIMPs likely compensate for loss of TIMP-3 activity and might also explain the absence of increased MMP activity in the retinae of *Timp-3$^{S156C/S156C}$* mice. These results suggest that the effect of S156C Timp-3 mutation on the MMP inhibitory function of the protein is tissue and cell type-specific.

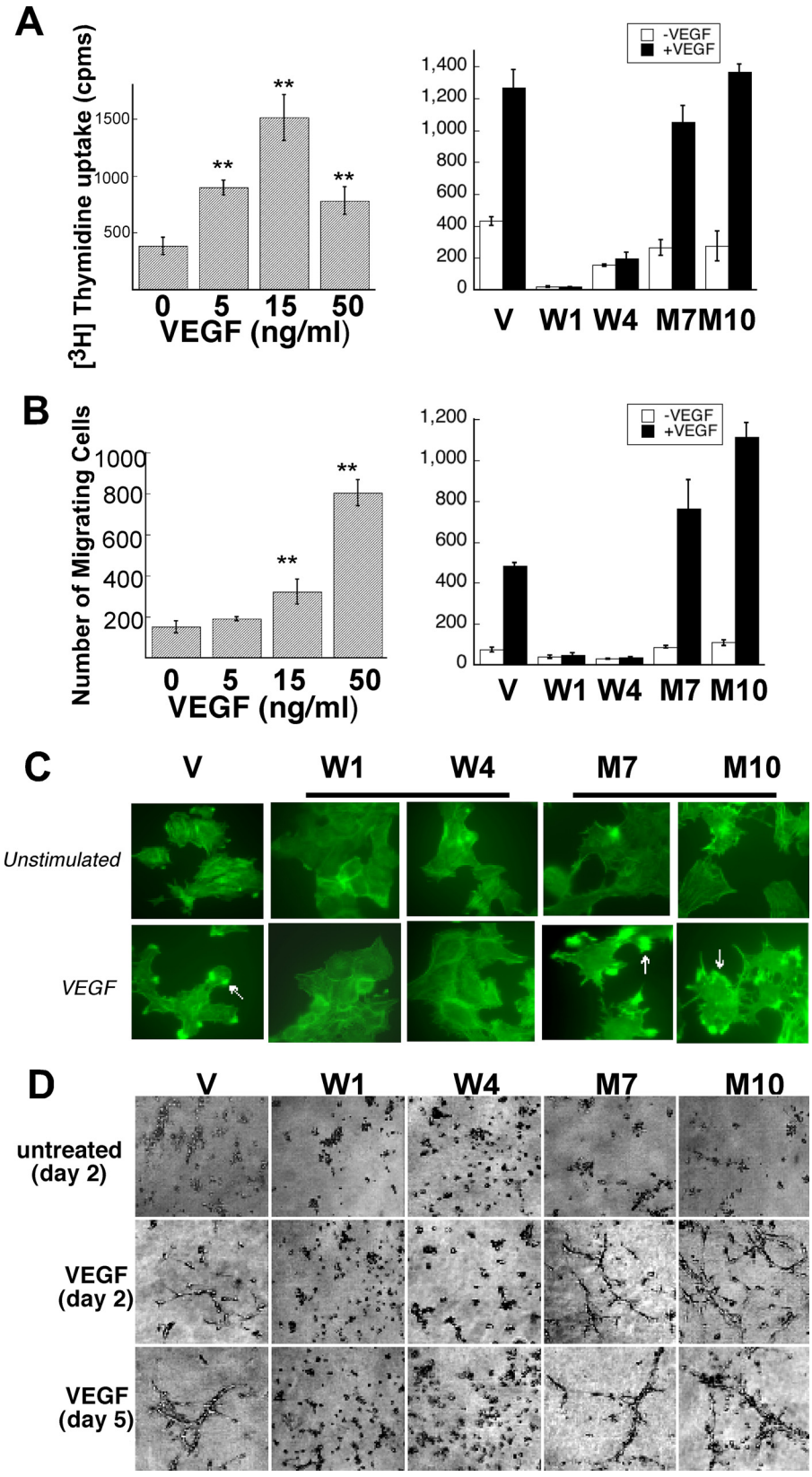

VEGFR-2 and phosphorylated VEGFR-2 (pVEGFR-2) levels were examined in the retina/choroid of mutant mice by immu-

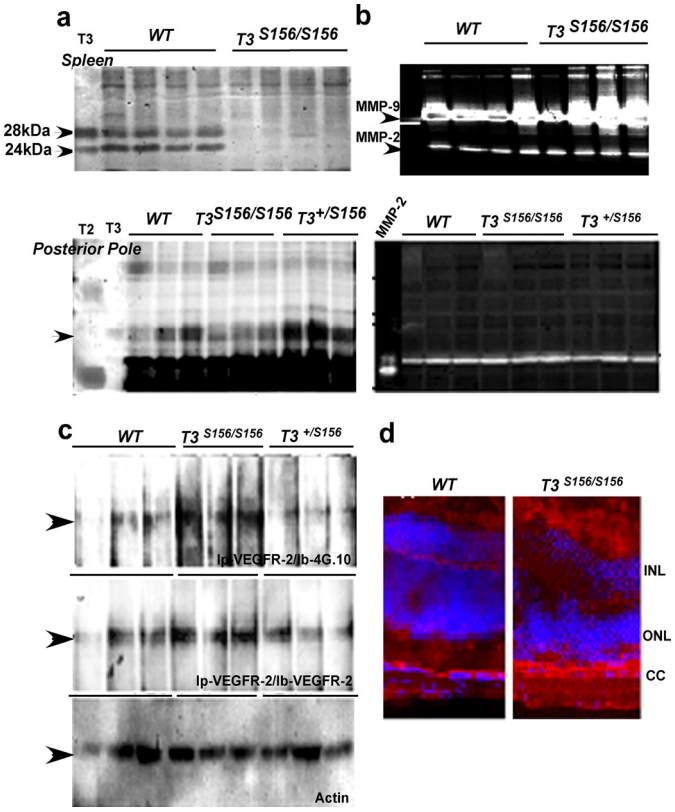

FIGURE 4. **Timp-3$^{S156C/S156C}$ mice have reduced TIMP-3 activity and increased expression of VEGFR-2.** Spleen (*a* and *b upper panels*) and retina/choroids (*a* and *b lower panels*) of *Timp-3*$^{+/+}$ (*WT*), *Timp-3*$^{S156C/S156C}$ (*KI*), or *Timp-3*$^{S156C/+}$ (*HET*) were subjected to reverse zymography (*a*) and zymography (*b*). Retina/choroid lysates were immunoprecipitated (*Ip*) with anti-VEGFR-2 antibodies (*c*) followed by Western blot analysis with anti VEGFR-2 antibodies (*middle panel*) or anti-phosphotyrosine antibody (*top panel*). Lysates were immunoblotted with antibodies to actin (*bottom panel*) to standardize for protein loading. *d*, cryosections from WT and T3$^{S156/S156}$ mouse eyes were analyzed by immunofluorescence staining with anti-VEGFR2 antibody using Texas Red-conjugated goat anti-mouse secondary antibody. *Red staining* indicated localization of VEGFR-2. *INL*, inner nuclear layer; *ONL*, outer nuclear layer; *CC*, choriocapillaris.

noprecipitation and Western blotting experiments. Increased expression of VEGFR-2 (Fig. 4*c*, *middle panel*) as well as phosphorylated VEGFR-2 (Fig. 4*c*, *upper panel*) was observed in the eyes of homozygous *TIMP-3*$^{S156C/S156C}$ relative to heterozygous *TIMP-3*$^{S156C/+}$ or wild-type mice. Immunofluorescence staining of mouse eyes with anti VEGFR-2 antibody revealed a stronger labeling of choriocapillaris from *Timp-3*$^{S156C/S156C}$ compared with wild-type littermates (Fig. 4*d*).

Increased VEGFR-2 in Human Eyes with Sorsby Fundus Dystrophy—To determine whether our results showing that mutant TIMP-3 causes an up-regulation of VEGFR-2 occurred in the human disease, we performed immunohistochemical analysis on a post-mortem eye of a 77-year-old woman with SFD. As described previously (24), the SFD eye showed an advanced stage of the disease with a marked loss of almost the entire photoreceptor layer and gliosis of the remaining retina (Fig. 5, *a* and *b*). The large deposits located between the RPE and elastin sublayer of the Bruch membrane were TIMP-3-positive (24) (Fig. 5*e*) and showed strong VEGFR-2 immunoreactivity (Fig. 5*g*). In the non-diseased normal eye TIMP-3 was localized to the Bruch membrane and the choriocapillary bed matrix as described previously (29) (Fig. 5*d*). Interestingly, we observed that TIMP-3 immunoreactivity was apparently reduced, whereas VEGFR-2 immunoreactivity was increased in the deposits underlying areas with RPE atrophy. Control tissues incubated with nonimmune mouse IgG in lieu of the anti TIMP-3 or VEGFR-2 antibody showed minimal background immunoreactivity (Fig. 5*h*).

DISCUSSION

SFD is a rare autosomal dominant, fully penetrant disease that commonly manifests as a hemorrhagic maculopathy secondary to choroidal neovascularization (12). The onset of symptoms typically occurs in the third to fifth decades of life with rapidly evolving loss of central vision or increasing nyctalopia (night blindness) over the course of several years (30, 31). The clinical features of SFD very closely resemble those of age-related macular degeneration, distinguished from each other primarily on the basis of age of onset of symptoms and family history. Given that mutations in TIMP-3 cause SFD, we reasoned it to be important to determine the role played by TIMP-3 protein in pathophysiological responses of the retina.

In this study we demonstrate that the expression of mutant S156C TIMP-3 in vascular endothelial cells augments VEGF-induced angiogenesis that is mediated by elevated levels and activation of functional surface VEGFR-2, which could potentially play a crucial role in the development of choroidal neovascularization in the disease. There has been an increasing debate on whether the SFD mutant TIMP-3 results in a loss of function, gain of function, or dominant-negative effect for the protein (32, 33).

The identification of TIMP-3 as an endogenous inhibitor of VEGFR-2-mediated angiogenesis (8) led us to postulate that S156C TIMP-3, a mutation that results in an earlier onset phenotype as well as prominent choroidal neovascularization, might be deficient in this angiogenesis inhibitory function. A recent report determined that recombinant S156C TIMP-3 retains its anti-angiogenic activities with its ability to block the binding of VEGF to VEFGR-2 and inhibit tube formation by mouse aortic endothelial cells in the fibrin bead assay (33). In

FIGURE 3. **S156C TIMP-3 is an inefficient inhibitor of VEGF-mediated EC proliferation, migration, and actin reorganization.** Serum-starved PAE$_{KDR}$ cells expressing WT (*W*) or S156C TIMP-3 (*M*) or vector alone (*V*) were incubated with or without VEGF and analyzed for proliferation, migration, actin reorganization, and tube formation. *A*, proliferation of endothelial cells in response to VEGF (15 ng/ml) for 40 h (*right panel*). [^{3}H]Thymidine incorporation was measured during the last 4 h of incubation. Optimal concentration of 15 ng/ml was determined from a dose-response curve generated using PAE$_{KDR}$ vector-transfected cells (*left panel*). $p < 0.01$ (**) and $p < 0.05$ (*) *versus* unstimulated controls. *B*, migration of endothelial cells toward VEGF (50 ng/ml) (*right panel*). Optimal concentration of 50 ng/ml was determined from a dose-response curve generated using PAE$_{KDR}$ vector-transfected cells (*left panel*). Migrating cell number is expressed as the means ± S.E. of quadruplicate samples. *C*, actin reorganization in PAE$_{KDR}$ cells stimulated with or without 50 ng/ml VEGF for 15 min at 37 °C. The *arrows* indicate membrane edge ruffling. Magnification ×1000. *D*, PAE$_{KDR}$ cells expressing WT (*W*) or S156C TIMP-3 (*M*) or vector alone (*V*) were cultured between two layers of type 1 collagen gel in the presence or absence of 50 ng/ml VEGF as indicated. Pictures were taken at the indicated times after inoculation. Images are of representative microscope fields (×200).

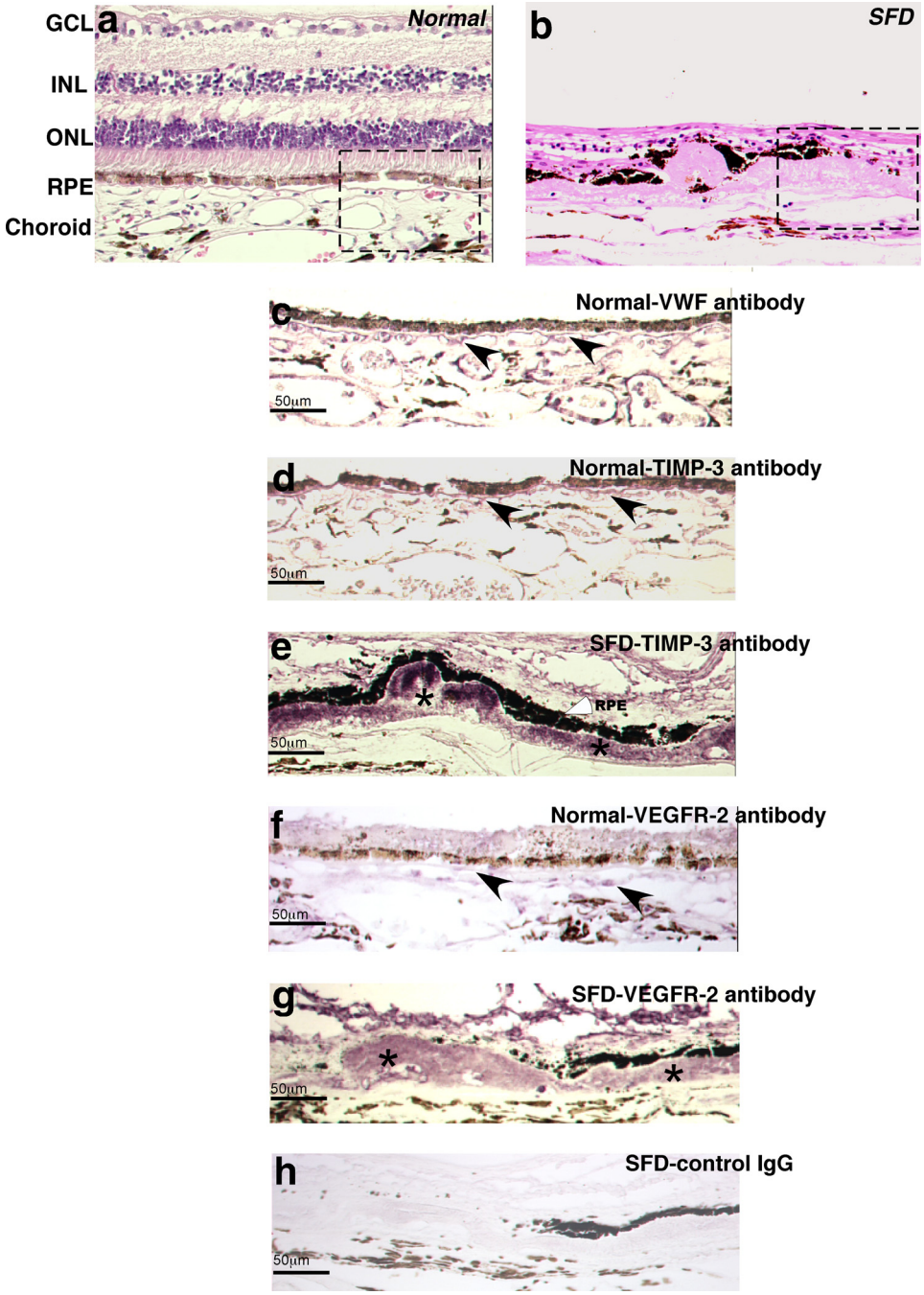

FIGURE 5. **Increased accumulation of VEGFR-2 in human SFD.** Paraffin embedded sections of a post-mortem human eye with SFD (*b*, *e*, *g*, and *h*) and an age-matched control non-diseased eye (*a*, *c*, *d*, *f*) were subjected to hematoxylin and eosin staining (*a* and *b*) immunohistochemistry with antibodies to VWF (*c*), TIMP-3 (*d* and *e*), VEGFR-2 (*f* and *g*) and control nonspecific IgG (*h*). *, sub-RPE deposits. *RPE*, retina pigment epithelium; *ONL*, outer nuclear layer; *INL*, inner nuclear layer; *GCL*, ganglion cell layer.

contrast, aortic endothelial cells from mice deficient in TIMP-3 showed a significantly increased tube formation and vessel outgrowth as well as VEGFR-2 downstream signaling (35). Interestingly, in our study S156C TIMP-3 expression resulted in an increase in the levels of the mature form of VEGFR-2 protein on the surface of endothelial cells. Elevated membrane-associated VEGFR-2 was sufficient to increase VEGF binding and subsequent VEGR-2 autophosphorylation and mitogen-activated protein kinase phosphorylation with downstream consequences of enhanced VEGF-dependent migration and tube formation *in vitro*. It should be noted that S156C TIMP-3 protein did not augment VEGF-dependent proliferation or the survival phase of *in vitro* angiogenesis. Because both recombinant TIMP-3 proteins (WT and S156C TIMP-3) can block the binding of VEGF to VEGR-2 (33), the loss of angio-inhibitory activity seen with mutant TIMP-3 in our study is most likely because of the up-regulation of the VEGFR-2, suggesting a gain of function. One possibility for the surprising findings in the present study is the use of ocular tissue from S156C *Timp-3* mutant mice as compared with liver and chondrocytes in the previous study (33). Our results suggest that in endothelial cells, S156C TIMP-3 shows reduced binding to the ECM and increased glycosylation. Whether this property of the mutant protein has a specific effect in the retina as a consequence of its interaction with unique matrix proteins in Bruch's membrane is currently being investigated.

The exact molecular mechanism by which S156C TIMP-3 increases membrane-associated VEGFR-2 is unknown. In PAE-KDR cells the VEGFR-2 protein is expressed under the control of the human cytomegalovirus promoter. The expression of mutant TIMP-3 results in an increase in membrane-bound VEGFR-2 protein in endothelial cells, whereas the relative amount of specific mRNA level remains stable, suggesting a post-transcriptional up-regulation of the receptor independent of the VEGFR-2 promoter, similar to that observed previously in PAE/KDR cells cultured under hypoxic conditions (27).

Pulse-chase experiments show that VEGFR-2 is initially synthesized as an immature 150-kDa protein and is rapidly glycosylated to a 200-kDa intermediate form and further glycosylated at a slower rate to a mature 230-kDa protein that is expressed on the cell surface (36). Our studies confirmed the presence of three VEGFR-2 isoforms in the plasma membrane of PAE_{KDR} cells. In addition to the mature protein, mutant TIMP-3 markedly increased the levels of the immature form compared with cells expressing WT TIMP-3. These data indicate that mutant TIMP-3 has distinctive effects on the early steps of maturation of the receptor. It has been

recently reported that novel highly efficient intrabodies can bind newly synthesized VEGFR-2 in the endoplasmic reticulum and block receptor transport to the cell surface (37, 38). It is an interesting possibility that WT and mutant TIMP-3 may differentially affect immature receptor translocation via distinct interactions with newly synthesized VEGFR-2 in the endoplasmic reticulum. In addition, it has been also suggested that β_3 integrin negatively regulates VEGFR-2 expression (39) and that caveolin plays a role in VEGFR-2 internalization (40). The role of TIMP-3 in these mechanisms is unknown.

The ADAMs family of membrane-spanning proteins combines features of both adhesion molecules and proteinases (41). ADAM17 (also known as tumor necrosis factor-α-converting enzyme), the sole mammalian cell surface-associated metalloproteinase sheddase so far identified, can affect the shedding of transmembrane-anchored proteins such as tumor necrosis factor-α (42), L-selectin (43), and interleukin-6 receptor (44) that are sensitive to TIMP-3. Recent studies have reported that recombinant S156C TIMP-3 protein can inhibit ADAM17 and aggrecan-cleaving MMPs (33). A TIMP-3-sensitive metalloproteinase also mediates the shedding of transmembrane protein syndecan-1 (45). Because VEGFR-2 can be proteolytically cleaved from endothelial cells (46) and SFD mutant TIMP-3 has attenuated MMP inhibitory activities, it is possible that mutant TIMP-3 could regulate the shedding of VEGFR-2 from endothelial cells. Taken together, these data indicate that the up-regulation of surface VEGFR-2 by mutant TIMP-3 is a dynamic process; the exact molecular mechanism(s) by which this occurs remains to be determined.

Ten independent mutations causing SFD have been identified to date. Seven of the 10 mutations introduce a new cysteine residue at the C terminus (S156C, G166C, G167C, Y168C, S170C, Y172C, and S181C). The E139*X* mutation, which introduces a stop codon at residue 139, results in an odd number of cysteine residues at the C terminus. The last two mutations, a mutation of the intron 4/exon 5 splice acceptor site as well as H158R mutation, do not create a new cysteine residue. Previous studies have reported that some TIMP-3 mutations gave rise to several additional higher molecular mass protein complexes (possibly TIMP-3 dimers) that retained their ability to inhibit MMPs and localized to the ECM when expressed in COS7 cells (17). Higher molecular weight complexes were also detected in mutant murine TIMP-3$^{S156C/S156C}$ fibroblast cells but lost their inhibitory activity (47). In contrast to these findings, we have detected a heavily glycosylated variant of mutant TIMP-3 protein with reduced MMP inhibitory activity and attenuated binding to the ECM in endothelial cells. The discrepancy between previous reports and ours is most likely because of differences in cell type examined. Reduced binding of mutant TIMP-3 to the ECM could be a result of an excessive glycosylation, which can potentially decrease its apparent affinity for the ECM, presumably by masking basic residues (16). Excessive glycosylation might also lead to a reduction of MMP inhibitory activity of mutant TIMP-3, presumably by a conformation change or reduced ECM binding (48). Indeed, our data have shown that the unglycosylated form of mutant TIMP-3 in the ECM, but not the glycosylated form in the conditioned medium, retained some MMP inhibitory activity. We have previously demonstrated that expression of S156C TIMP-3 in human RPE cell line results in reduced inhibition of MMPs and increased activation of MMP2 and MMP9 (10). More recently, the inability of the S156C mutation to inhibit MT1-MMP activation of pro-MMP2 has been confirmed independently in addition to the finding of accumulation of a turnover-resistant fraction of mutant TIMP-3 protein in RPE cells (26). Examination of the choriocapillaris and sub-RPE deposits in mice expressing mutant TIMP-3 and in an SFD human eye confirms the presence of increased VEGFR-2 protein.

In summary, we have shown that SFD S156C mutation specifically and dynamically up-regulates surface VEGFR-2 level and activity resulting in enhanced VEGF-dependent angiogenesis. This points to a novel mechanism for the regulation of angiogenesis by S156C TIMP-3 in SFD. Systemic bevacizumab has been recently shown to be a promising treatment option for choroidal neovascularization in a patient with SFD (34). Our data also show that S156C TIMP-3 is highly glycosylated, soluble, and inefficient in MMP inhibitory activity, suggesting that in addition to anti VEGF therapies, MMP inhibitors might provide therapeutic benefit.

REFERENCES

1. Apte, S. S., Olsen, B. R., and Murphy, G. (1995) *J. Biol. Chem.* **270,** 14313–14318
2. Pavloff, N., Staskus, P. W., Kishnani, N. S., and Hawkes, S. P. (1992) *J. Biol. Chem.* **267,** 17321–17326
3. Ahonen, M., Poukkula, M., Baker, A. H., Kashiwagi, M., Nagase, H., Eriksson, J. E., and Kähäri, V. M. (2003) *Oncogene* **22,** 2121–2134
4. Baker, A. H., Zaltsman, A. B., George, S. J., and Newby, A. C. (1998) *J. Clin. Invest.* **101,** 1478–1487
5. Bond, M., Murphy, G., Bennett, M. R., Amour, A., Knauper, V., Newby, A. C., and Baker, A. H. (2000) *J. Biol. Chem.* **275,** 41358–41363
6. Fata, J. E., Leco, K. J., Voura, E. B., Yu, H. Y., Waterhouse, P., Murphy, G., Moorehead, R. A., and Khokha, R. (2001) *J. Clin. Invest.* **108,** 831–841
7. Mannello, F., and Gazzanelli, G. (2001) *Apoptosis* **6,** 479–482
8. Qi, J. H., Ebrahem, Q., Moore, N., Murphy, G., Claesson-Welsh, L., Bond, M., Baker, A., and Anand-Apte, B. (2003) *Nat. Med.* **9,** 407–415
9. Della, N. G., Campochiaro, P. A., and Zack, D. J. (1996) *Invest. Ophthalmol. Vis. Sci.* **37,** 1921–1924
10. Qi, J. H., Ebrahem, Q., Yeow, K., Edwards, D. R., Fox, P. L., and Anand-Apte, B. (2002) *J. Biol. Chem.* **277,** 13394–13400
11. Fariss, R. N., Apte, S. S., Olsen, B. R., Iwata, K., and Milam, A. H. (1997) *Am. J. Pathol.* **150,** 323–328
12. Sorsby, A., and Mason, M. E. (1949) *Br. J. Ophthalmol.* **33,** 67–97
13. Barbazetto, I. A., Hayashi, M., Klais, C. M., Yannuzzi, L. A., and Allikmets, R. (2005) *Arch. Ophthalmol.* **123,** 542–543
14. Felbor, U., Benkwitz, C., Klein, M. L., Greenberg, J., Gregory, C. Y., and Weber, B. H. (1997) *Arch. Ophthalmol.* **115,** 1569–1571
15. Felbor, U., Stöhr, H., Amann, T., Schönherr, U., and Weber, B. H. (1995) *Hum. Mol. Genet* **4,** 2415–2416
16. Langton, K. P., Barker, M. D., and McKie, N. (1998) *J. Biol. Chem.* **273,** 16778–16781
17. Langton, K. P., McKie, N., Curtis, A., Goodship, J. A., Bond, P. M., Barker, M. D., and Clarke, M. (2000) *J. Biol. Chem.* **275,** 27027–27031
18. Lin, R. J., Blumenkranz, M. S., Binkley, J., Wu, K., and Vollrath, D. (2006) *Am. J. Ophthalmol.* **142,** 839–848
19. Tabata, Y., Isashiki, Y., Kamimura, K., Nakao, K., and Ohba, N. (1998) *Hum. Genet.* **103,** 179–182
20. Weber, B. H., Vogt, G., Pruett, R. C., Stöhr, H., and Felbor, U. (1994) *Nat. Genet.* **8,** 352–356
21. Holz, F. G., Haimovici, R., Wagner, D. G., and Bird, A. C. (1994) *Retina* **14,** 329–334
22. Jacobson, S. G., Cideciyan, A. V., Regunath, G., Rodriguez, F. J., Vanden-

burgh, K., Sheffield, V. C., and Stone, E. M. (1995) *Nat. Genet.* **11,** 27–32
23. Kalmus, H., and Seedburgh, D. (1976) *J. Med. Genet.* **13,** 271–276
24. Fariss, R. N., Apte, S. S., Luthert, P. J., Bird, A. C., and Milam, A. H. (1998) *Br. J. Ophthalmol.* **82,** 1329–1334
25. Majid, M. A., Smith, V. A., Easty, D. L., Baker, A. H., and Newby, A. C. (2002) *FEBS Lett.* **529,** 281–285
26. Langton, K. P., McKie, N., Smith, B. M., Brown, N. J., and Barker, M. D. (2005) *Hum. Mol. Genet.* **14,** 3579–3586
27. Waltenberger, J., Mayr, U., Pentz, S., and Hombach, V. (1996) *Circulation* **94,** 1647–1654
28. Weber, B. H., Lin, B., White, K., Kohler, K., Soboleva, G., Herterich, S., Seeliger, M. W., Jaissle, G. B., Grimm, C., Reme, C., Wenzel, A., Asan, E., and Schrewe, H. (2002) *Invest. Ophthalmol. Vis. Sci.* **43,** 2732–2740
29. Kamei, M., and Hollyfield, J. G. (1999) *Invest. Ophthalmol. Vis. Sci.* **40,** 2367–2375
30. Capon, M. R., Polkinghorne, P. J., Fitzke, F. W., and Bird, A. C. (1988) *Eye* **2,** 114–122
31. Polkinghorne, P. J., Capon, M. R., Berninger, T., Lyness, A. L., Sehmi, K., and Bird, A. C. (1989) *Ophthalmology* **96,** 1763–1768
32. Li, Z., Clarke, M. P., Barker, M. D., and McKie, N. (2005) *Expert Rev. Mol. Med.* **7,** 1–15
33. Fogarasi, M., Janssen, A., Weber, B. H., and Stöhr, H. (2008) *Matrix Biol.* **27,** 381–392
34. Prager, F., Michels, S., Geitzenauer, W., and Schmidt-Erfurth, U. (2007) *Acta Ophthalmol. Scand.* **85,** 904–906
35. Janssen, A., Hoellenriegel, J., Fogarasi, M., Schrewe, H., Seeliger, M., Tamm, E., Ohlmann, A., May, C. A., Weber, B. H., and Stöhr, H. (2008) *Invest. Ophthalmol. Vis. Sci.* **49,** 2812–2822
36. Takahashi, T., and Shibuya, M. (1997) *Oncogene* **14,** 2079–2089
37. Böldicke, T., Weber, H., Mueller, P. P., Barleon, B., and Bernal, M. (2005) *J. Immunol. Methods* **300,** 146–159
38. Böldicke, T. (2007) *J. Cell Mol. Med.* **11,** 54–70
39. Reynolds, L. E., Wyder, L., Lively, J. C., Taverna, D., Robinson, S. D., Huang, X., Sheppard, D., Hynes, R. O., and Hodivala-Dilke, K. M. (2002) *Nat. Med.* **8,** 27–34
40. Labrecque, L., Royal, I., Surprenant, D. S., Patterson, C., Gingras, D., and Béliveau, R. (2003) *Mol. Biol. Cell* **14,** 334–347
41. Blobel, C. P. (1997) *Cell* **90,** 589–592
42. Black, R. A., Rauch, C. T., Kozlosky, C. J., Peschon, J. J., Slack, J. L., Wolfson, M. F., Castner, B. J., Stocking, K. L., Reddy, P., Srinivasan, S., Nelson, N., Boiani, N., Schooley, K. A., Gerhart, M., Davis, R., Fitzner, J. N., Johnson, R. S., Paxton, R. J., March, C. J., and Cerretti, D. P. (1997) *Nature* **385,** 729–733
43. Borland, G., Murphy, G., and Ager, A. (1999) *J. Biol. Chem.* **274,** 2810–2815
44. Hargreaves, P. G., Wang, F., Antcliff, J., Murphy, G., Lawry, J., Russell, R. G., and Croucher, P. I. (1998) *Br. J. Haematol.* **101,** 694–702
45. Fitzgerald, M. L., Wang, Z., Park, P. W., Murphy, G., and Bernfield, M. (2000) *J. Cell Biol.* **148,** 811–824
46. Ebos, J. M., Bocci, G., Man, S., Thorpe, P. E., Hicklin, D. J., Zhou, D., Jia, X., and Kerbel, R. S. (2004) *Mol. Cancer Res.* **2,** 315–326
47. Soboleva, G., Geis, B., Schrewe, H., and Weber, B. H. (2003) *J. Cell. Physiol.* **197,** 149–156
48. Butler, G. S., Apte, S. S., Willenbrock, F., and Murphy, G. (1999) *J. Biol. Chem.* **274,** 10846–10851

S156C Mutation in Tissue Inhibitor of Metalloproteinases-3 Induces Increased Angiogenesis

Jian Hua Qi, Ganying Dai, Philip Luthert, Shyam Chaurasia, Joe Hollyfield, Bernhard H. F. Weber, Heidi Stöhr and Bela Anand-Apte

J. Biol. Chem. 2009, 284:19927-19936.
doi: 10.1074/jbc.M109.013763 originally published online May 28, 2009
